

UDC 542.06+546.05

DOI: 10.15372/CSD20180508

Influence of Alumina Nanoparticles on Transformation of Mechanically Activated Gibbsite into α -Al₂O₃

G. R. KARAGEDOV

*Institute of Solid State Chemistry and Mechanochemistry, Siberian Branch, Russian Academy of Sciences, Novosibirsk, Russia**E-mail: garik@solid.nsc.ru*

Abstract

Mechanical activation of gibbsite containing 0.5–5 vol. % of alumina nanoparticles was carried out in a planetary mill. It was demonstrated that upon 10g acceleration and above, subsequent calcination at 800 °C resulted in the complete transformation of aluminium hydroxide into a stable modification of alumina with particle size below 100 nm. Thermal treatment of activated aluminium hydroxide in wet media inhibits aggregate formation. Furthermore, powder-compacted samples are sintered till densities higher than 98 % of theoretically possible at 1350 °C.

Key words: aluminium hydroxide, α -alumina, nanopowder, synthesis, sintering

INTRODUCTION

Due to a combination of good hardness, chemical inertness, availability, and efficiency, alumina is most demanded as a ceramic material. Nevertheless, its use is held back by poor cracking resistance (3–4.5 MPa · m^{0.5}) and sensibility to erosive and abrasive impact. A fundamental cause of poor strength of Al₂O₃-based materials is anisotropy of thermomechanical properties of stable crystal α -modification characterised by the hexagonal structure of the unit cell. When the material is formed by high-temperature sintering in the cooling step, chaotically oriented crystals (grains) turn out to be uncorrelated with differently oriented neighbours according to thermal expansion coefficients. As a result, there are intergranular microstresses, the value of which is proportional to the grain size.

Modern methods to increase Al₂O₃-based materials strength are based on reducing technology microstresses due to grain size preservation in the nano-range [1]. That requires the use of

initial ceramic powders with the minimum particle size.

New methods to produce such powders envisage the precipitation of gels containing inoculating α -Al₂O₃ nanocrystals, [2–4], the preparation of the organic matrix to separate growing oxide particles [5–8], gel freezing [9], the use of catalysts [10], mechanochemical synthesis, etc. [11]. Nevertheless, all of them have not found practical use on an industrial scale so far.

For example, low-temperature calcination of gels containing seed nanoparticles allows producing ceramic powders of exceptionally high quality that are able to ensure a density of a material sintered at a temperature of 1300 °C (instead of the traditional 1600–1800 °C) more than 98 % of the theoretically possible while maintaining the grain size of 0.1–0.2 μ m. Nevertheless, large scale production of alumina (around 500 t/year only for the needs of the military-industrial complex) is economically impractical. There is no current industrial production of sufficiently pure aluminium nitrate or aluminum oxalate of at the re-

quired scale in Russia. Furthermore, even the theoretical mass yield of α - Al_2O_3 from aluminum nitrate is just 13–14 %, whereas that from aluminum oxalate is 16–17 %, which naturally makes alumina cost higher.

On the other side, a number of enterprises on aluminum hydroxide production (alumina content of 65 %) are functioning in Russia, due to which it is relevant to explore the effect of seed crystals and other techniques developed in salt sources on the crystallization of alumina from $\text{Al}(\text{OH})_3$.

The initial aluminum hydroxide is completely transformed into α -alumina at temperatures not lower than 1200 °C, which inevitably results in the formation of coarsely dispersed powders. Attempts to reduce the crystallization temperature of α - Al_2O_3 from $\text{Al}(\text{OH})_3$ by introducing seed particles into boehmite sol were made as early as in 1985. The authors of [12] succeeded in lowering the crystallization temperature to 1050 °C to produce a powder with particle sizes in the 0.1–0.4 μm range. Whereas in [13], when 10 % of pseudoboehmite was added, a powder with a narrow distribution of particle size in the 0.2–0.3 μm range was produced. As noted in [14], treatment of the Bayer method-derived aluminum hydroxide in a mill (apparently, roll) by Al_2O_3 balls facilitates reducing the transition temperature into the α -modification to 1100 °C and the formation of particles in 0.45–0.7 μm size range. The authors associate this grinding media wear that reaches 23 % of the treated material and according to the authors, is a source of seed particles. For a planetary mill, mechanical activation (MA) of above 15g of gibbsite containing 1–5 % of alumina particles with a size 25 nm reduces the temperature of complete transformation into the α -phase to 800–850 °C, whereas crystallite size of the generated powder is 0.050 μm [15].

Moreover, it was demonstrated that intensive MA of gibbsite causing its amorphization even with the lack of seed crystals leads to a decrease in the α - Al_2O_3 crystallization temperature [16–18] up to 900 °C upon certain thermal treatment conditions. According to high-resolution electron microscopy (HREM) data [19], 2–3 nm domains with α - Al_2O_3 structure are formed in activated gibbsite. In such a way, the effect of an increase in crystallization temperature and therefore product particles is apparently identical with the effect of seed particles.

It is worth noting that MA of γ -alumina with steel or tungsten carbide balls in planetary mills

leads to direct transformation of aluminum oxide into the stable α -modification [20, 21], however, the development of this method is unlikely due to pollutions inevitable here.

Unfortunately, there is no data regarding the purity of the synthesized α - Al_2O_3 or its successful use to produce ceramics in none of the noted papers. Therefore one may suggest only the presence of the qualitative effect of seed crystals *versus* α - Al_2O_3 crystallization.

EXPERIMENTAL

The research work used finely dispersed aluminium hydroxide (manufacture of BaselCement CJSC, TU 1711-046-00196368-95) and analytically pure aluminum hydroxide (Donetsk Plant of Chemical Reagents, GOST 118418-76); α - Al_2O_3 nanopowders with an average particle size of about 20 or 50 nm produced according to methods described in [22] and [15], respectively, were used as a seed. The seed was mixed with $\text{Al}(\text{OH})_3$ in certain proportions; 7 g of the mixture was exposed to mechanical processing in the AGO-2M mill using drums and balls made of zirconium dioxide, the ratio of the loading mass to the mass of the balls was 20 : 1 (Table 1).

If it was required to produce media of high moisture content, powders were calcined in a LAC 04/17 or Carbolite 15/180 furnace after mechanical treatment. The heating rate was 5 °C/min.

The resulting powders were pressed into tablets with a diameter of 16 mm and a height of 3–4 mm at a pressure of 30 MPa by dry uniaxial pressing followed by isostatic compression at a pressure of 200–250 MPa on the AIP3-12-60C plant (American Isostatic Press, USA). After pressing, the samples were sintered in air inside a LAC 04/17 furnace at a heating rate of 5 °C/min and an isothermal exposure of 1.5 h. The density of the resulting ceramics was determined by the Archimedes method according to GOST 20018-74.

X-ray phase analysis of powders and crystallite size determination was carried out using a DRON-4 X-ray diffractometer with the $\text{CuK}_{\alpha 1}$ radiation and a graphite monochromator, and also with a Bruker D8 Advance diffractometer with a step of 0.02° and an accumulation time of 0.2 s. The crystallite sizes, coherent scattering regions (CSR), in powders and grains in sintered materials were determined using PowderCell 2.4 or TOPAS software with the required introduc-

TABLE 1

Transition degree into α - Al_2O_3 and particle size *versus* mechanical activation conditions

Acceleration, <i>g</i>	Time, min	Ball diameter, mm	Amount of introduced seed, %	Transition degree into α -phase, %	Calcination temperature, °C	CSR size, nm
25	20	10	5	100	800	45
25	20	10	5 (50 nm)	100	870	80
20	20	10	5	100	800	53
20	20	10	5 (15 nm)	100	850	57
15	20	10	5	100	800	50
15	20	10	1	100	850	90
15	20	3	5	100	850	55
10	20	10	3	100	850	60
7.5	20	5	5	-70	850	69
5	20	5	5	-85	900	88
5	20	5	5	-80	850*	97
5	20	10	5	-70	870	81
1	180	15-20	5	-50	930	N/D
1	400	15-20	5	-50	930	N/D
Mortar	30	-	5	-30	900	N/D

Note. CSR is coherent scattering regions; N/D indicates not determined.

*Sample is produced in media of high moisture content.

tion of reference samples produced under identical survey conditions. The results for both programs match with an accuracy of a few nanometers. If the X-ray diffraction pattern had other phases, in addition to α - Al_2O_3 , its content was roughly evaluated according to the ratio of peak areas attributed therein towards the other ones.

Electron micrographs were acquired using Hitachi 3400 SN and JEM2000FX2 microscopes. The powder was pretreated with ultra sound in a slightly acidic aqueous solution (pH ~ 3.5).

RESULTS AND DISCUSSION

Figure 1 gives X-ray diffraction patterns of the initial aluminum hydroxide calcined at 800 °C and mechanically activated species. It can be seen that the X-ray diffraction pattern of unactivated $\text{Al}(\text{OH})_3$ does not have α -modification reflections, whereas after treatment with 20*g*, this is the only phase except for a hardly apparent peak of the δ -phase (indicated with an arrow in the figure). A less intensive activation with 15*g* yields a mix-

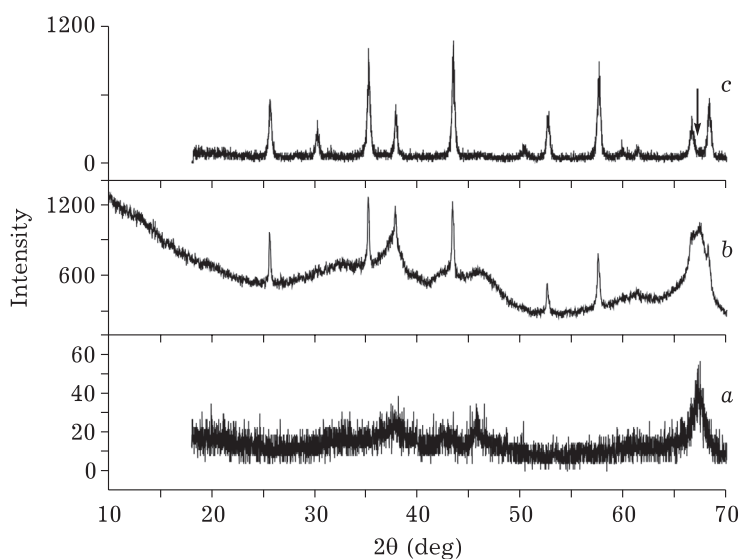


Fig. 1. X-Ray diffraction patterns of the initial aluminum hydroxide calcined at 800 °C (a) and activated species with 15*g* (b) and 20*g* (c).

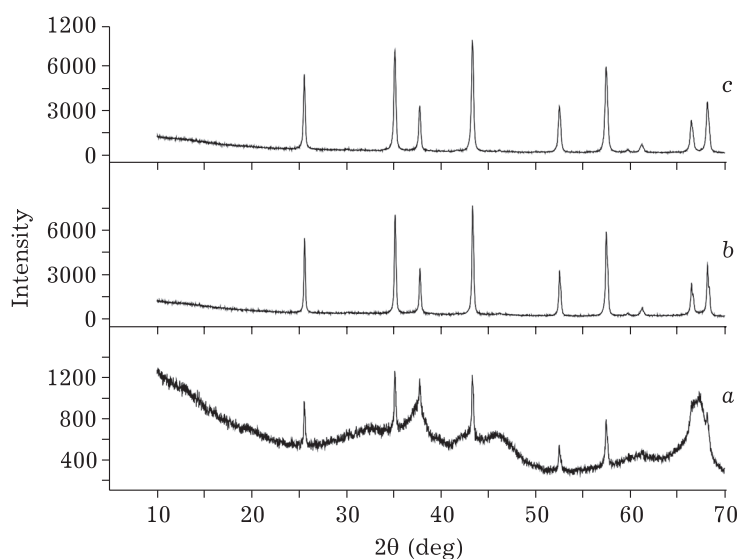


Fig. 2. X-ray diffraction patterns of aluminum hydroxide activated with 15g and calcined at 800 °C, free of (a) and containing 0.5 (b) and 5 % of seed particles (b).

ture of the α -phase and intermediate modifications of Al_2O_3 . However, if small amounts of seed nanoparticles are added to $\text{Al}(\text{OH})_3$ powder treated with 15g, even at such a low temperature, one may produce the 100 % phase (Fig. 2).

It is obvious that the particle size of the product produced at this temperature is significantly lower than that after standard calcination at 1200 °C, *i.e.* around 50 nm instead of 3–4 μm . Table 1 gives some typical data acquired under different MA conditions. As can be seen, mechanical treatment intensity in our experiments is no less than 10g. When intensities are lower, one fails to carry out complete transformation into $\alpha\text{-Al}_2\text{O}_3$ at temperatures smaller than 900 °C (the generated powder is comprised of particles with

a size of lower than 100 nm precisely at these temperatures). When using a seed with a greater size (50 nm), product particles are approximately twice bigger, too. However, they correspond to the nano range.

Figure 3 demonstrates the amount of the introduced particle. Accepting that seed particles act as α -phase crystallization sites, then a decrease in product particle size is qualitatively understandable with an increase in the number of these centres. Nevertheless, it is impossible to determine the number of centres generated resulting of MA not knowing how many embryos are artificially introduced.

Thuswise, upon an increase in seed amount from 0.5 to 5 %, *i.e.* by ten times, crystallite size had to decrease in $\sqrt[3]{10} = 2.16$ times, whereas in reality, it was decreased by 1.5 times. The same amount of crystallization centres, as when introducing around 1.5 % of the seed is likely to be generated resulting from MA.

During low-temperature calcination of $\text{Al}(\text{OH})_3$ activated with seed particles, the monophasic product is generated, its crystallite size being almost comparable with that for powders produced from aluminium oxalate or aluminium nitrate [4, 15].

Nevertheless, its behaviour during sintering differs significantly. Table 2 gives data regarding the densities of samples compacted by dry pressing and sintered. It can be seen that unlike mechanically activated aluminium hydroxide, aluminium salts-produced powders have exceptionally high densities for specified temperatures and

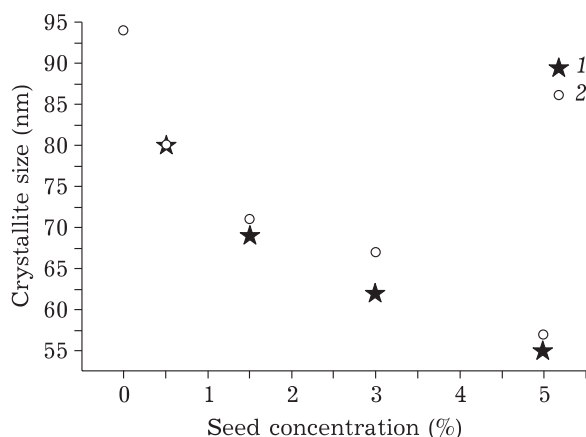


Fig. 3. Alpha-alumina crystallite size versus amounts of $\alpha\text{-Al}_2\text{O}_3$ seed particles in gibbsite activated with 15g and calcined at 800 (1) and 900 °C (2).

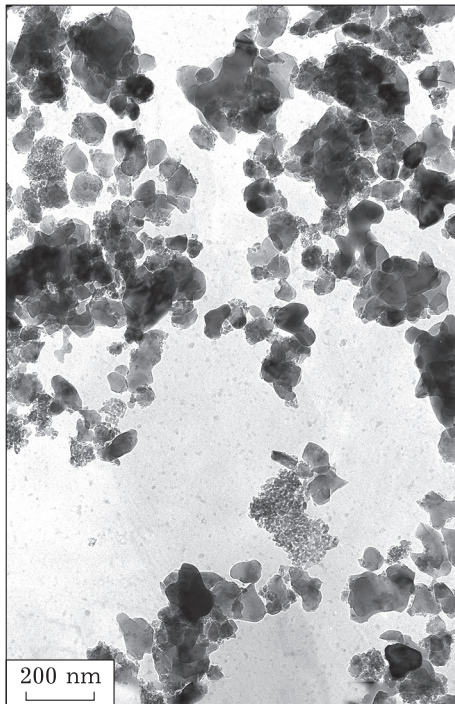


Fig. 4. Electron microscopic image of aluminum hydroxide containing 3 % of seed particles activated with 15g and calcined in air at 800 °C.

therefore the submicron microstructure with good mechanical properties. Moreover, an increase in sintering temperature to 1500 °C does not facilitate a substantial rise in density.

As can be seen in the electron micrograph of the powder produced with 15g of $\text{Al}(\text{OH})_3$ with 3 % of the seed (Fig. 4), alongside with small particles (50–70 nm), there are relatively large aggregates (over 200 nm) with particles that are closely stuck together and probably recrystallized. Materials generated from such powders do not usually reach high densities when sintering [23].

Assuming that the formation of dense aggregates from Al_2O_3 proceeds during calcination due to their binding among themselves *via* oxygen bridges

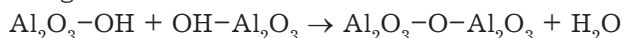


TABLE 2

Crystallite size of and the sintering behaviour of powders of aluminium salts and $\text{Al}(\text{OH})_3$

Initial components	Phase composition	Crystallite size, nm	Density at 1300–1350 °C, % of theoretically possible
$\text{Al}(\text{NO}_3)_3 + 4$ % seed	100 % α - Al_2O_3	60–80	98
$\text{Al}_2(\text{C}_2\text{O}_4)_3 + 3$ % seed	100 % α - Al_2O_3	95	98
$\text{Al}(\text{OH})_3 + 0.5$ – 5 % seed	100 % α - Al_2O_3	60–80	89–92
$\text{Al}(\text{OH})_3 + 0$ % seed	100 % α - Al_2O_3	95	86

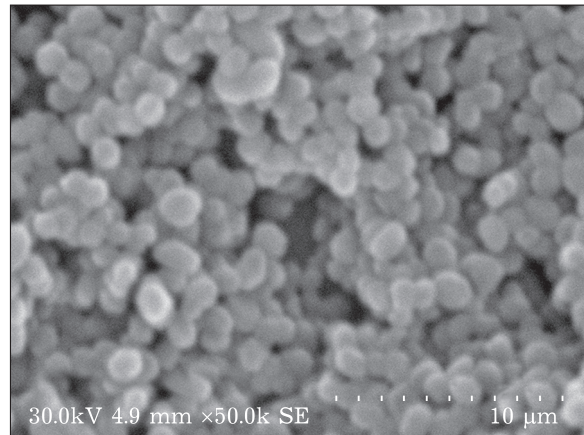


Fig. 5. Electron microscopic image of aluminum hydroxide activated with 15g and calcined in media of high moisture content at 800 °C.

then, according to the Le Chatelier principle, the equilibrium may be shifted to the left, having increased the pressure of water vapours during the process.

Figure 5 shows the photograph of the powder with 3 % contents of seed particles. The powder is activated with 15g and calcined in humid air with a water vapour pressure greater than 10 kPa. In comparison with Fig. 4, the crystallites in the powder have a somewhat greater size, the round shape, and narrow size distribution, and also there are no large aggregates. Due to compacting by the dry isostatic pressing of this powder at 200 MPa, the sample that sinters in air at 1350 °C to a density of 3.91 g/cm³, *i.e.* to that greater than 98 % of theoretically possible value, has been produced.

CONCLUSION

Relatively gentle mechanical treatment of gibbsite in a planetary mill at $\geq 10g$ accelerations together with a small amount of α - Al_2O_3 nanoparticles facilitates product formation. The material completely passes into the stable α -modification

with crystallite size of below 100 nm already at 800 °C. Herewith, the powder is partially aggregated and therefore uncured blanks compacted therefrom do not reach high densities upon sintering. Thermal treatment of activated powders in media with elevated water vapour pressure allows avoiding particle aggregation and almost non-porous materials are generated already at a sintering temperature of 1350 °C.

Acknowledgements

The research was supported by the Integrated program of the Siberian Branch of the Russian Academy of Sciences “Integration and development” (project 63.2).

REFERENCES

- 1 Krell A., Klimke J., Hutzler T., *J. Eur. Ceram. Soc.* 2009. Vol. 29. P. 275–281.
- 2 Karagedov G. R., Myz A. L., Lyakhov N. Z., *Materialoved.* 2011. Vol. 9. P. 36–45.
- 3 Karagedov G. R., Myz A. L., Kichay V., *Khim. Ust. Razv.* 2016. Vol. 24, No. 2. P. 157–162.
- 4 Karagedov G. R., Myz A. L., *Materialoved.* 2017. Vol. 8. No. 34–38.
- 5 Pati R. K., Ray J. C., Pramanik P., *J. Am. Ceram. Soc.* 2001. Vol. 84. P. 2849–2852.
- 6 Das R. N., Bandyopadhyay A., Bose S., *J. Am. Ceram. Soc.* 2001. Vol. 84. P. 2421–2423.
- 7 Lin C.-P., Wen S.-B., Lee T.-T., *J. Am. Ceram. Soc.* 2002. Vol. 85. P. 129–133.
- 8 Lee Y.-C., Wen S.-B., Wenglin L., Lin C.-P., *J. Amer. Ceram. Soc.* 2007. Vol. 90. P. 1723–1727.
- 9 Zeng W., Rabelo A. A., Tomasi R., *Key Eng. Mat.* 2001. Vol. 189–191. P. 16–20.
- 10 Dudnik E. V., Shevchenko A. V., Ruban A. K., Redko V. P., Lopato L. M., *Powder Metallurgy and Metal Ceramics.* 2008. Vol. 47. P. 379–383.
- 11 Sanxu Pu, Lu Li, Ji Ma, Fuliang Lu, Jianguo Li, *Sci. Reports.* 2015. Vol. 5. P. 11575.
- 12 Kumagai M., Messing G., *J. Am. Ceram. Soc.* 1985. Vol. 68. P. 500–505.
- 13 Yang Y., Jiao X., Chen B., *J. Nanopart. Res.* 2013. Vol. 15. P. 221855.
- 14 Xie Z.-P., Lu J.-W., Huang Y., Cheng Y.-B., *Mater. Letters.* 2003. Vol. 57. P. 2501–2508.
- 15 Karagedov G. R., *Chem. Sust. Dev.* 2011. Vol. 19, No. 1. P. 77–83.
- 16 Yamaguchi G., Sakamoto K., *Bull. Chem. Soc. Japan.* 1959. Vol. 32. P. 121364–1368.
- 17 MacKenzie K. J. D., Temuujin J., Okada K., *Thermochim. Acta.* 1999. Vol. 327. P. 103–108.
- 18 Jang S.-W., Lee H.-Y., Lee S.-M., Lee S. W., Shim K.-B., *J. Mat. Sci. Let.* 2000. Vol. 19. P. 507–510.
- 19 Yong C. C., Wang J., *J. Am. Ceram. Soc.* 2001. Vol. 84. P. 1225–30.
- 20 Bokhonov B. B., Konstanchuk I. G., Boldyrev V. V., *Mater. Res. Bull.* 1995. Vol. 30. P. 1277–84.
- 21 Poluboyarov V. A., Andryushkova O. V., Pauli I. A., Korotaeva Z. A., *Vliyaniye Mekhanicheskikh Vozdeystviy na Fiziko-Khimicheskiye Protssesy v Tverdykh Telakh*, Izdvo NGTU, 2011.
- 22 RU Pat. No. 2392226, 2010.
- 23 Lange F. F., *J. Am. Ceram. Soc.* 1984. Vol. 67. P. 83–89.